Journal of Hazardous Materials 185 (2011) 1045–1052

Contents lists available at ScienceDirect

Journal of Hazardous Materials

journal homepage: www.elsevier.com/locate/jhazmat

Adsorption of acid dyes from aqueous solutions by the ethylenediamine-modified magnetic chitosan nanoparticles

Limin Zhou[a,b,*], Jieyun Jin[a], Zhirong Liu[b], Xizhen Liang[a], Chao Shang[a]

[a] State Key Laboratory Breeding Base of Nuclear Resources and Environment, East China Institute of Technology, Nanchang, 330013, PR China
[b] Key Laboratory of Radioactive Geology and Exploration Technology Fundamental Science for National Defense, East China Institute of Technology, Fuzhou 344000, PR China

ARTICLE INFO

Article history:
Received 8 August 2010
Received in revised form 4 October 2010
Accepted 4 October 2010
Available online 28 October 2010

Keywords:
Chitosan nanoparticles
Magnetic
Ethylenediamine
Adsorption
Acid Orange 7
Acid Orange 10

ABSTRACT

The adsorption characteristics of Acid Orange 7(AO7) and Acid Orange 10 (AO10) from aqueous solutions onto the ethylenediamine-modified magnetic chitosan nanoparticles (EMCN) have been investigated. The EMCN were essentially monodispersed and had a main particle size distribution of 15–40 nm and saturated magnetization of 25.6 emu/g. The adsorption experiments indicated that the maximum adsorption capacity occurred at pH 4.0 for AO7 and pH 3.0 for AO10, respectively. Due to the small diameter and the high surface reactivity, the adsorption equilibrium of AO7 and AO10 onto the EMCN reached very quickly. Equilibrium experiments fitted well with the Langmuir isotherm model, and the maximum adsorption capacity of the EMCN at 298 K was determined to be 3.47 mmol/g for AO7 and 2.25 mmol/g for AO10, respectively. Thermodynamic parameters such as enthalpy change (ΔH°), free energy change (ΔG°) and entropy change (ΔS°) were estimated and the results indicated that the adsorption process was spontaneous and exothermic. Furthermore, the EMCN could be regenerated through the desorption of the dyes in NH_4OH/NH_4Cl solution (pH 10.0) and could be reused to adsorb the dyes again.

1. Introduction

Most of dyes released during textiles, clothing, printing, and dyeing processes are considered as hazardous and toxic to some organisms and may cause allergic dermatitis, skin irritation, carcinogenic and mutagenic to human and aquatic organisms [1]. However, these dyes in wastewaters are difficult to remove, because they have recalcitrant molecules (particularly azo dyes with an aromatic structure), are resistant to aerobic digestion, and are stable to oxidizing agents. Several techniques are available for the treatment of the dyes such as an electrochemical technique destroying the colour groups [2], a bio-degradation process mineralising the colourless organic intermediates [3], chemical oxidation including homogeneous and heterogeneous photocatalytic oxidation [4,5]. Among the many techniques of dye removal, adsorption is the procedure of choice and gives the best results as it can be used to remove different types of dyes [6,7].

Adsorption of different dyes has been studied using low cost adsorbents such as activated carbon [8], kaolin [9], montmorillonite clay [10], waste red mud [11], Fullers earth and fired clay [12]. Currently chitosan is being greatly exploited because it is relatively cheap and exhibit higher adsorption capacities [13,14]. Chitosan is a cationic biopolymer obtained from alkaline N-deacetylation of chitin, the second most abundant biopolymer in nature. Chitosan exhibits a higher adsorption capacity and faster adsorption rate of anionic dye pollutants than many conventional adsorbents due to the presence of large amounts of amino ($-NH_2$) groups [13]. In acidic solution, the amino groups of chitosan are easily protonated and can bind anionic dye anions. Chitosan resins are highly selective, efficient and easily regenerable relative to other adsorbent materials. The use of chitosan resins for the removal of dyes from aqueous solutions was recently reported by several authors [6,14–17].

Chitosan is usually needed to be cross-linked to improve its chemical stability in acid media. Although the crosslinking method may enhance the resistance of chitosan against acids, the process may reduce its adsorption capacity of dyes, especially when the crosslinking procedure involves in the reaction of amino groups, which are expected to play a great part in the adsorption process. In order to improve the adsorption capacity and selectivity of dyes, a number of chitosan derivates have been obtained by grafting functional groups such as acrylic and acrylamide [14], poly(methylmethacrylate) [15], poly(alkyl methacrylate) [16], and vinyl acetate [17] through a crosslinked chitosan back bone.

Most of the chitosan-based adsorbents were submicron to micron-sized and need large internal porosities to ensure adequate surface area for adsorption. However, the diffusion limitation within the particles led to the decreases in the adsorption rate

* Corresponding author at: Key Laboratory of Radioactive Geology and Exploration Technology Fundamental Science for National Defense, East China Institute of Technology, Fuzhou 344000, PR China. Tel.: +86 794 8829625; fax: +86 794 8258320.
E-mail address: minglzh@sohu.com (L. Zhou).

0304-3894/$ – see front matter © 2010 Elsevier B.V. All rights reserved.
doi:10.1016/j.jhazmat.2010.10.012

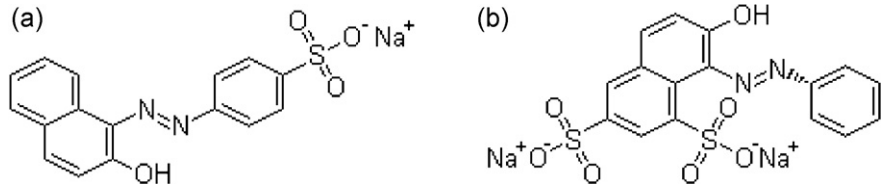

Fig. 1. The structures of (a) Acid Orange 7 (AO7) and (b) Acid Orange 10 (AO10).

and available capacity. Compared to the traditional micron-sized supports used in separation process, nano-sized adsorbents possess quite good performance due to high specific surface area and the absence of internal diffusion resistance [18,19]. However, the nano-adsorbents could not be separated easily from aqueous solution by filtration or centrifugation. Magnetic nano-adsorbents can be manipulated by an external magnetic field and hence facilitate phase separation.

Several studies have indicated that $-NH_2$ groups in chitosan are the main sites for the adsorption of dyes containing D-SO_3^- groups through ionic interactions of the colored dye ions with the protonated amino groups on the chitosan [6,13,14]. In this work, the magnetic chitosan nanoparticles (MCN) were prepared and then modified with ethylenediamine (EMCN) to increase the $-NH_2$ active groups and thus enhance the adsorption capacity for acid dyes. The adsorption behaviour of the EMCN toward Acid Orange 7 and Acid Orange 10 was studied. The equilibrium isotherms and thermodynamic parameters were determined and discussed.

2. Experimental

2.1. Chemicals and reagents

Chitosan with 40 mesh, 90% degree of deacetylation and molecular weight of 1.3×10^5 was purchased from Yuhuan Ocean Biology Company (Zhejiang, China). Glutaraldehyde, epichlorohydrine, ethylenediamine, Acid Orange 7 and Acid Orange 10 were supplied by Aldrich and Sigma Chemical, and were used without any further purification. All the other reagents used in this work were of analytical grade. The structures of dye Acid Orange 7 and Acid Orange 10 are presented in Fig. 1, and the chemical characteristics of them are listed in Table 1.

2.2. Preparation and characterization of the adsorbents

The preparation of ethylenediamine-modified magnetic chitosan nanoparticles (EMCN) has been reported in our previous work [19]. The magnetic chitosan nanoparticles (MCN) were prepared by adding the basic precipitant of NaOH solution into a W/O microemulsion system containing chitosan and ferrous salt. The MCN were then treated with epichlorohydrine and grafted with ethylenediamine to obtain the EMCN.

The dimension and morphology of the EMCN were observed by transmission electron microscopy (TEM) (Hitachi, H-800). Magnetization measurements were preformed with VSM (Princeton Applied Research, model-155). Thermalgravimetric analysis was conducted on Shimadzu TGA-50H with heating rate of 10 K/min. The concentration of the amine active sites in the obtained resins was estimated using the volumetric method [20].

2.3. Uptake measurements

2.3.1. Effect of pH

Uptake experiments were performed at controlled pH and 298 K by shaking 50 mg of EMCN with 50 mL (5×10^{-3} mol/L) dye solution for 1.5 h at 200 rpm. The solution pH was adjusted to the desired value by adding either nitric acid or sodium hydroxide standardized solutions. After mixing, the aqueous phase was separated from the solid phase by magnetic settlement and centrifugation at 12,000 rpm. The residual concentration of dyes was determined at the maximum wavelength (484 nm for AO7 and 475 nm for AO10) using a Cary 50 UV–vis spectrophotometer (Varian, USA).

2.3.2. Effect of time

The experiments were conducted by shaking 300 mg EMCN with 300 mL (5×10^{-3} mol/L) dye solution at the optimum pH values (pH 4.0 for AO7 and pH 3.0 for AO10). The contents of the flask were agitated on a shaker at 200 rpm and 298 K. Several milliliters of the solution was taken at different time intervals, where the residual concentrations of dyes were calculated after the volume correction.

2.3.3. Adsorption isotherms

Complete adsorption isotherms were obtained by placing 50 mg of EMCN in a series of flasks containing 50 mL dye solution at definite concentrations and the optimum pH values. The flasks were agitated on a shaker at 200 rpm and definite temperatures (298, 308, and 318 K) for 1.5 h. After adsorption, the residual concentration of the dyes in the solution was determined. The amount of dyes adsorbed per unit of sorbent mass calculated by the mass balance equation.

2.3.4. Desorption and reuse after desorption

For the desorption studies, 300 mg of EMCN were loaded with the AO7 or AO10 using 300 mL of 5×10^{-3} mol/L dye solution at optimum pH (the adsorption procedure is same as Section 2.3.2). The dye-loaded EMCN were collected and washed with distilled water to remove any unadsorbed dyes, and then were agitated with 300 mL of NH_4OH/NH_4Cl (pH 10.0) for 2 h. To investigate the reusablity of the adsorbents, the EMCN after desorption was reused in adsorption experiments and the process was repeated for three times.

3. Results and discussion

3.1. Characterization of EMCN

The TEM micrograph (Fig. 2) showed that the EMCN were essentially monodispersed and had a main particle size distribution of 15–40 nm. The magnetization measurement performed with VSM

Table 1
The chemical characteristics of the dyes.

Generic name	Abbreviation	Chromophore	Formula weight	Maximum wavelength λ_{max} (nm)
C.I. Acid Orange 7	AO7	Monoazo	350.32	484
C.I. Acid Orange 10	AO10	Anthraquinone	452.38	475

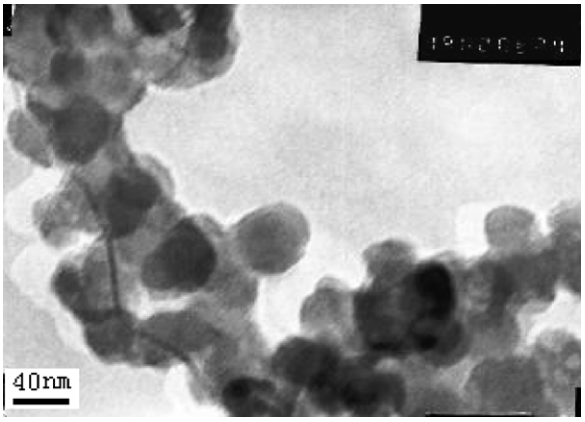

Fig. 2. TEM micrograph for EMCN, the bar is 40 nm.

(Fig. 3) indicated that the saturation magnetization of the EMCN was 25.6 emu/g. As mentioned in a previous report, this magnetic susceptibility value is sufficient for this resin to be used in wastewater treatment [21]. Meanwhile, the insert figure in Fig. 3 indicated that nanoparticles had the characteristics of superparamagnetism. It's also found that when a magnet with a surface magnetization of 3000 G was near the bottle, the chitosan nanoparticles suspended in the solution will aggregate within 1–2 min. The large saturation magnetization makes the EMCN be easily seperated by the external magnetic field. The average mass content of Fe_3O_4 in the EMCN by TGA was about 33.5%, as calculated from the TGA data at 873 K. As shown in the FTIR spectra of the EMCN, the peaks at 560–660 cm^{-1} were assigned to Fe–O bond vibration of Fe_3O_4. The carbonyl bands at around 1630 cm^{-1} indicate that chitosan reacts with glutaraldehyde to form *Schiff* base. The increase of absorption intensity of the peak at 2920 cm^{-1} for the EMCN compared to the MCN should be attributed to the introduction of C–H in epichlorohydrine in the synthesis of the EMCN. The concentration of the amine active sites of the MCN and EMCN was determined to be 2.4 mmol/g and 3.8 mmol/g, respectively. These results indicated that MCN had been modified with ethylenediamine successfully.

3.2. Effect of pH

The influence of pH on the adsorption of AO7 and AO10 onto the EMCN for pH ranging 2–10 is illustrated in Fig. 4. It can be seen that the maximum uptake value for AO7 and AO10 was obtained at pH 4.0 and pH 3.0, respecitively (the optimum pH values selected for the further experiments). The observed decrease in the uptake value at low pH (less than the optimum pH values) may be attributed to the decrease in dye dissociation which leads to a lower concentration of the anionic dye species available to interact with the resin's active sites. Above the optimum pH values, the EMCN displays a sharp decrease in the uptake value as pH increases. This behaviour can be explained on the basis of the lower extent of protonation of amino groups at high pH.

The mechanisms of the adsorption process of the acid dyes (AO7 and AO10) on the EMCN are likely to be the ionic interactions of the colored dye ions with the amino groups of the EMCN. In aqueous solution, the acid dyes are first dissolved and the sulfonate groups of acid dye (D-SO_3Na) dissociate and are converted to anionic dye ions.

$$\text{D-SO}_3\text{Na} \rightarrow \text{D-SO}_3^- + \text{Na}^+$$

Also, in the presence of H^+, the amino groups of the EMCN (R-NH_2) became protonated.

$$\text{R-NH}_2 + \text{H}^+ \leftrightarrow \text{R-NH}_3^+$$

The adsorption process then proceeds due to the electrostatic attraction between these two oppositely charged ions

$$\text{R-NH}_3^+ + \text{D-SO}_3^- \leftrightarrow \text{R-NH}_3^+ \ldots {}^-\text{SO}_3\text{-D}$$

The point of zero charge for the EMCN was found to be 4.8 using standard potentiometric method. Therefore, the surface charge of the EMCN is positively charged at pH < 4.8. It seems that at pH 3–4, most of –NH_2 groups are protonated, which are favorable for the adsorpion of anionic dyes. However, at high pH, the number of protonated –NH_2 groups will decrease and more OH^- ions will be available to compete with the anionic sulfonic groups, therefore the adsorption capacity for the acid dyes decreases at high pH.

3.3. Effect of contact time

Fig. 5 shows the effect of contact time on the adsorption capacity (Q, mmol/g) of AO7 and AO10 by the EMCN. The results demonstrate that the adsorption for both dyes is rapid. In the case of AO7, the maximum adsorption is attained in 40 min, while for AO10 it takes 60 min, after which the change in the removal percentage is insignificant. The contact time of 1.5 h was found to be sufficient to reach equilibrium, and so it was selected in further experiments.

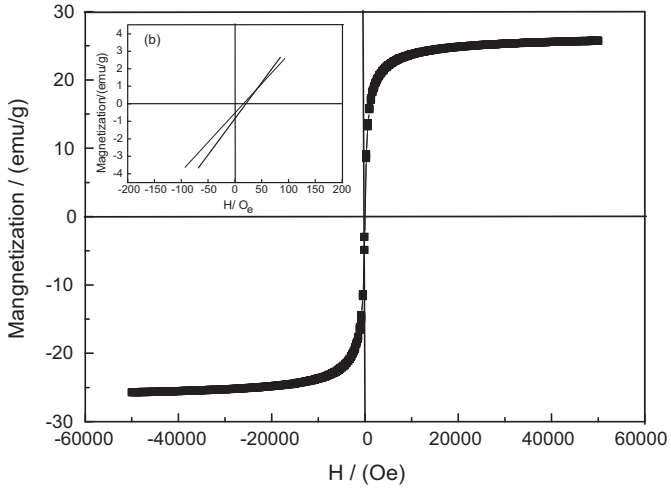

Fig. 3. VSM of EMCN.

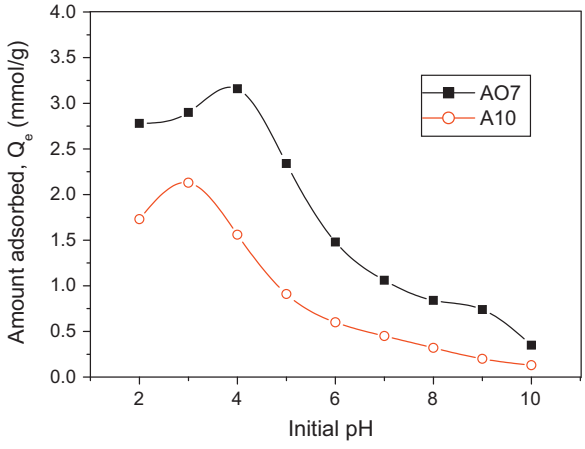

Fig. 4. Effect of pH on the adsorption of AO7 and AO10 on EMCN (initial concentration 5×10^{-3} mmol/L, EMCN 1.0 g/L, shaking rate 200 rpm, 298 K). The symbols represent the average values of two tests under the identical conditions with error <5%.

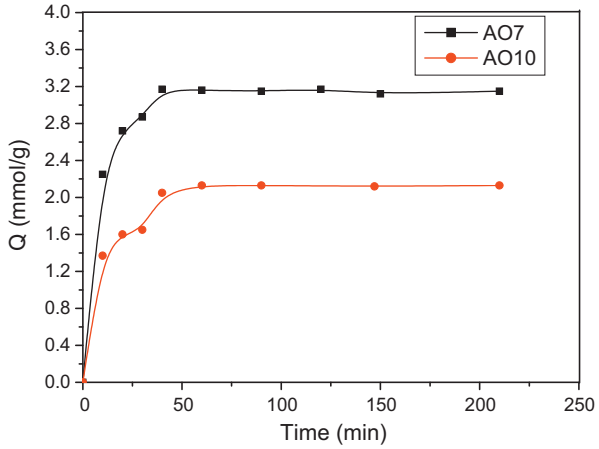

Fig. 5. Effect of adsorption time on the uptake of AO7 and AO10 by EMCN (initial concentration 5×10^{-3} mmol/L, EMCN 1.0 g/L, shaking rate 200 rpm, 298 K). The symbols represent the average values of two tests under the identical conditions with error < 5%.

It was reported that a long time is needed to attain equilibrium for dyes with several adsorbents, such as GLA and H_2SO_4-crosslinked chitosan resin [6], chitosan/kaolin/γ-Fe_2O_3 composites [7], and other adsorbents [8–12,14]. In contrast, in the present study, AO7 and AO10 are adsorbed in a short time (no more than 1 h). This can be attributed to the large surface area, the sufficient exposure of active sites and the high surface reactivity of the magnetic chitosan nanoparticles.

3.4. Adsorption isotherms

Fig. 6 shows the adsorption isotherms of AO7 and AO10 on the EMCN at different temperatures. The equilibrium adsorption capacity of the dye (Q_e) increased with increasing of the dye concentration. The adsorption curves indicate that the uptake of both dyes decreases with increasing temperature. The adsorption isotherms were studied using three isotherm models:

Langmuir isotherm equation [22]:

$$\frac{C_e}{Q_e} = \frac{C_e}{Q_m} + \frac{1}{Q_m K_L} \quad (1)$$

Freundlich isotherm equation [23]:

$$\ln Q_e = b_F \ln C_e + \ln K_F \quad (2)$$

and Dubinin-Radushkevich (D-R) isotherm equation [24]:

$$\ln Q_e = K\varepsilon^2 + \ln Q_{D-R} \quad (3)$$

where C_e is the equilibrium concentration of the dye (mmol/L); Q_e is the adsorbed value of dyes at equilibrium concentration (mmol/g); K_L is the Langmuir binding constant which is related to the energy of adsorption (L/mmol); K_F and b_F are the Freundlich constants related to the adsorption capacity and intensity, respectively. Q_m and Q_{DR} are the Langmuir and D-R maximum adsorption capacities of the dye (mmol/g), respectively; K is the D-R constants; ε is the Polanyi potential given as Eq. (4) [25]:

$$\varepsilon = RT \ln\left(1 + \frac{1}{C_e}\right) \quad (4)$$

where R is the gas constant (8.314 J/(K mol), and T is the temperature (K). The D-R constant (K) can give the valuable information regarding the mean energy of adsorption by Eq. (5) [26]:

$$E = (-2K)^{-1/2} \quad (5)$$

where E is the mean adsorption energy. The results were shown in Table 2. The Langmuir isotherm was found to fit quite well with the experimental data for both AO7 and AO10 in accordance with the linear correlation coefficients (R^2). This indicates the homogeneity of active sites on the surface of the EMCN. It is notable that the EMCN is a composite adsorbent which is composed of chitosan and Fe_3O_4. However, chitosan was mainly responsible for the adsorption of the dyes, therefore, it is reasonable that the EMCN can provide the homogeneity of active sites. The difference in the values of K_L for AO7 and AO10 refers the different binding strength and capacity of the dyes with the surface of the EMCN.

The Langmuir maximum adsorption capacity (Q_m) of AO7 (2.82–3.47 mmol/g) at different temperatures (298–318 K) was much higher than that of AO10 (1.79–2.25 mmol/g). The difference in the degree of adsorption may be attributed to the size and chemical structure of the dye molecule. AO7 has the smaller molecular size and has only one sulfonate acid group (monovalent). The smaller molecular size of AO7 not only increases the concentration of dye on the surface of the chitosan particle but also enables a deeper penetration of dye molecules into the internal pore structure of the EMCN. The monovalent nature of AO7 dye molecules makes more protonated amino groups on the chitosan particle available for the adsorption of dye molecules. It also reduces the electrostatic repulsion of adjacent dye molecules, which is significant in the nano-scale EMCN, on the adsorbent surface when compared with divalent dye molecule such as AO10, enabling dye molecules to be packed more closely on the adsorbent surface.

The maximum adsorption capacity (Q_m) of the EMCN obtained by Langmuir isotherm for AO7 and AO10 adsorption at 298 K was 3.47 and 2.25 mmol/g, respectively, which is higher than that of the unmodified magnetic chitosan microspheres (2.65 mmol/g for AO7 and 1.76 mmol/g for AO10) obtained in the same conditions as in the EMCN. These results indicated that chemical modification of magnetic chitosan nanoparticles with ethylenediamine improved the adsorption capacity for both AO7 and AO10 due to the higher concentration of active sites of the EMCN.

In addition, the mean adsorption energy (E) from the D-R isotherm, defined as the free energy change when one mole of ion is transferred from infinity in solution to the surface of the solid, could be used to estimate the type of adsorption. The adsorption behaviour could be predicted as the physical adsorption in the range of 1–8 kJ/mol and the chemical adsorption in more than 8 kJ/mol [25]. The E values (Table 2) of 8.53–9.29 kJ/mol for AO7 and 8.41–9.66 kJ/mol for AO10 indicated that the adsorption of both dyes onto the EMCN was predominant on the chemisorption process.

It is also important to compare the value of maximum adsorption capacity obtained from this study with values from other reported low-cost adsorbents, since this will suggest the effectiveness of the EMCN as potential adsorbent for dyes treatment. The adsorption capacities for acid dyes (AO7 and AO10) using the EMCN are comparable to those using other chitosan adsorbents as shown in Table 3. It was notable that only 66.5 wt% of chitosan was responsible for the adsorption of the AO7 and AO10 dyes. The maximum adsorption capacity based on the weight of chitosan was 5.12 mmol/g (1827 mg/g) for AO7 and 3.38 mmol/g (1530 mg/g) for AO10, respectively. The high adsorption capacity of the EMCN for the dyes might be reasonably referred to the high specific surface area of magnetic chitosan nanoparticles with a much smaller diameter, leading to almost all active sites available.

The degree of suitability of the obtained resins towards dyes was estimated from the values of the separation factor (R_L) using the following relation [31].

$$R_L = \frac{1}{1 + K_L C_0} \quad (6)$$

where K_L is the Langmuir equilibrium constant and C_0 is the initial concentration of dye. Values of $0 < R_L < 1$ indicates the suitability of

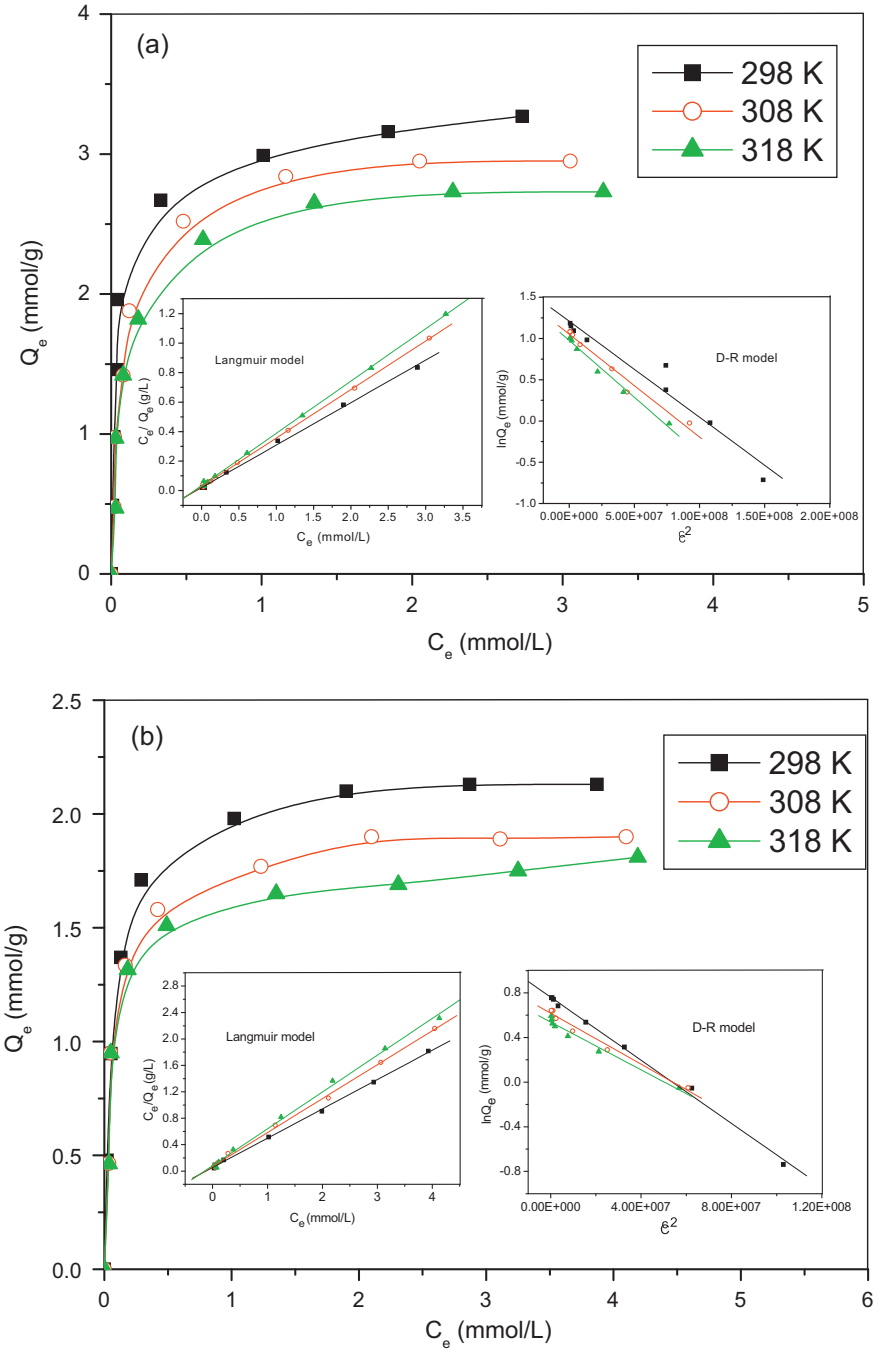

Fig. 6. Adsorption isotherms of the adsorption of (a) AO7 and (b) AO10 dyes on the EMCN at different temperatures (initial concentration 0.5–6 mmol/L, EMCN 1.0 g/L, shaking rate 200 rpm, 298–318 K). The symbols represent the average values of two tests under the identical conditions with error <5%.

Table 2
Langmuir, Freundlich and Dubinin-Radushkevich isotherm constants and correlation coefficients.

Dye	Temperature (K)	Langmuir			Freundlich			Dubinin-Radushkevich			E (kJ/mol)
		Q_m (mmol/g)	K_L (L/mmol)	R^2	K_F (mmol/g)	b_F	R^2	$Q_{D\text{-}R}$ (mmol/g)	$K \times 10^{-8}$ (J^2/mol^2)	R^2	
AO7	298	3.47	13.71	0.9980	2.97	0.2762	0.8057	3.34	−1.161	0.9751	9.29
	308	3.04	12.14	0.9997	2.61	0.3021	0.8336	2.86	−1.246	0.9855	8.96
	318	2.82	10.33	0.9995	2.34	0.2963	0.8009	2.65	−1.375	0.9919	8.53
AO10	298	2.25	8.08	0.9989	1.81	0.2516	0.8401	2.14	−1.415	0.9980	8.41
	308	1.94	7.22	0.9981	1.59	0.2347	0.7815	1.85	−1.143	0.9900	9.35
	318	1.79	6.63	0.9967	1.47	0.2172	0.7620	1.71	−1.071	0.9868	9.66

Table 3
Comparison of adsorption capacities of dyes on different chitosan-based adsorbents.

Adsorbent	Dye	Q_{max} (mg/g)	Reference
EMCN	C.I. Acid Orange 7	1215 (3.47 mmol/g)	This work
EMCN	C.I. Acid Orange 10	1017 (2.25 mmol/g)	This work
Chitosan-GLA	Acid Red 37	167	[27]
Chitosan-GLA	Acid Blue 25	127	[27]
Chitosan particles	Acid Green 25	645	[28]
Chitosan particles	Acid Orange 10	923	[28]
Chitosan particles	Acid Orange 12	973	[28]
Chitosan-ECH	Metanil Yellow	1334	[29]
Chitosan-ECH	Reactive Blue 15	722	[29]
Chitosan hydrobeads	Congo red	93	[30]
Carboxyl groups grafted chitosan	Basic Yellow 37	595	[14]
PMMA grafted chitosan	Procion Yellow MX 8G	277	[15]
PMMA grafted chitosan	Remazol Brilliant Violet	384	[15]

the process. The values of R_L for the EMCN toward the adsorption of AO7 and AO10 for all concentration ranges (0.5–6.0 mmol/L) at 298–318 K lie between 0.012–0.162 and 0.020–0.231 respectively. This indicates the suitability of the EMCN for both AO7 and AO10 adsorption.

3.5. Thermodynamic of AO7 and AO10 adsorption

It is known that values of thermodynamic parameters such as enthalpy change (ΔH°), entropy change (ΔS°) and free energy change (ΔG°) must be taken into consideration in order to determine the spontaneity of a process. In this study, the thermodynamic parameters of the adsorption process are obtained from experiments at various temperatures (298–318 K). The values of K_L (Table 2) at different temperature were processed according to the following van't Hoff equation [32] to obtain the thermodynamic parameters of the adsorption process

$$\ln K_L = \frac{-\Delta H^\circ}{RT} + \frac{\Delta S^\circ}{R} \quad (7)$$

where ΔH° and ΔS° are enthalpy and entropy changes, respectively, R is the universal gas constant (8.314 J/mol K) and T is the absolute temperature (in Kelvin). Plotting $\ln K_L$ against $1/T$ gives a straight line with slope and intercept equal to $\Delta H^\circ/R$ and $\Delta S^\circ/R$, respectively. The values of ΔH° and ΔS° were calculated from Fig. 7 and reported in Table 4. The negtive values of ΔH° indicate the exothermic nature of adsorption process. The positive values of ΔS° suggest the increased randomness during the adsorption of AO7 and AO10. The source of this entropy gain is due to liberation of water molecules from the hydrated shells of the sorbed species [25]. Gibbs free energy of adsorption (ΔG°) was calculated from the following relation and aslo given in Table 4.

$$\Delta G^\circ = \Delta H^\circ - T\Delta S^\circ \quad (8)$$

The negative values of ΔG° for both dyes indicate that the adsorption on the EMCN is a spontaneous process, whereby no energy input from outside of the system is required. However, the values of ΔG° decreased with increasing temperature, suggesting that adsorption of AO7 and AO10 onto the EMCN became less favourable at higher temperature [6]. As the temperature increases,

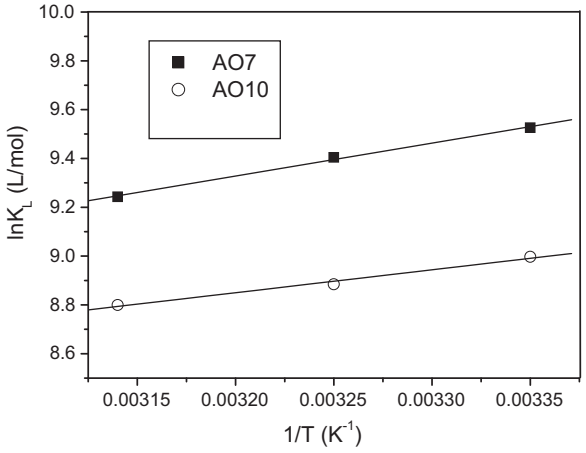

Fig. 7. van't Hoff plots for the uptake of AO7 and AO10 dyes on the EMCN.

the mobility of dye molecules increases, causing the molecules to escape from the solid phase to the liquid phase. Therefore, the amount of AO7 and AO10 that can be adsorbed will decrease. The increase mobility of dye molecules at elevated temperature may also be reflected in the values of K_L (Table 2). The values of K_L for both dyes decrease as the temperature increases, indicating lower affinity of the resins towards the dyes at higher temperature.

3.6. Desorption and reuse

The capacities of the EMCN for the AO7 and AO10 dyes in the adsorption–desorption–adsorption cycles were shown in Fig. 8. It may be observed that at the first adsorption step, the adsorption capacities for the AO7 and AO10 dyes reached the values of 3.16 and 2.13 mmol/g, respectively. After the desorption step, the adsorbed AO7 and AO10 dyes were removed about 81.1% and 87.8%, respectively, by NH_4OH/NH_4Cl solution at pH 10. This could be ascribed to the fact that, in the basic solution, the positively charged amino groups were deprotonated and the electrostatic interaction between chitosan and dye molecules became much weaker. The second and the third adsorption step revealed the similar dynam-

Table 4
Thermodynamic parameters of AO7 and AO10 adsorption by the EMCN.

Dye	Temperature (K)	ΔG° (kJ/mol)	$T\Delta S^\circ$ (kJ/mol)	ΔH° (kJ/mol)	ΔS° (J/mol)
AO7	298	−23.63	12.48	−11.14	41.90
	308	−24.35	13.21		
	318	−25.10	13.96		
AO10	298	−22.29	14.48	−7.81	48.59
	308	−23.08	15.27		
	318	−23.89	16.09		

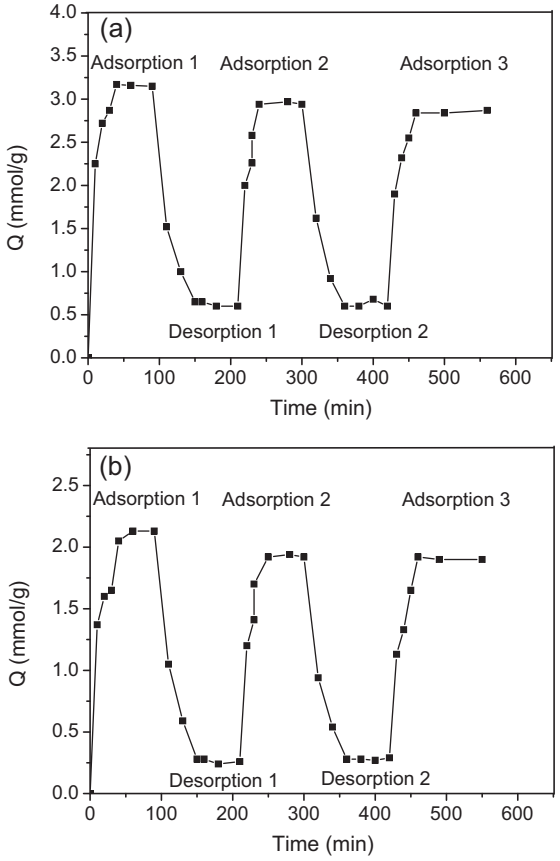

Fig. 8. Absorption–desorption cycles of (a) AO7 and (b) AO10 dyes on the EMCN.

ical shape of the first adsorption step. It can also be seen that the total adsorption capacities of both AO7 and AO10 dyes for the second and the third step maintain more than 90% of those for the first adsorption step. Therefore, the EMCN can be reused for further dye adsorption.

4. Conclusion

This research have demonstrated that the EMCN can be used for the effective adsorption of AO7 and AO10 from aqueous solution. The interest in using the EMCN for removal or recovery of dyes from aqueous solutions is related to their unique characteristics, such as very large surface area and high surface reactivity. In addition, the EMCN is easily seperated by the external magnetic field, by this way the problem of phase seperation using the traditional adsorbents can be resolved. The EMCN exhibited good kinetic characteristics (equilibrium time 40 min for AO7 and 60 min for AO10) and high adsorption loading capacities for AO7 and AO10 (i.e., 3.47 and 2.25 mmol/g at 298 K, respectively). The EMCN also showed good improvements in the uptake properties of AO7 and AO10 compared to unmodified ones. The maximum adsorption capacity occurred at around pH 4.0 for AO7 and pH 3.0 for AO10. Equilibrium experiments fitted well the Langmuir isotherm model and the adsorption capacity decreases with increasing temperature. The EMCN showed higher adsorption capacity for AO7 than for AO10 due to the size and chemical structure of the dye molecule. In addition, the mean adsorption energy from the Dubinnin-Radushkevich isotherms revealed that the adsorption process was predominant on the chemisorption process. Thermodynamic calculation indicated that the adsorption process was spontaneous and exothermic. Furthermore, the EMCN could be regenerated using NH_4OH/NH_4Cl solution at pH10 and could be reused to adsorb the dyes again.

Acknowledgments

This work was supported by the Science & technology Pillar Program of Jiangxi, China (No. 2009BSB08600), and the scientific research fund from the Education Bureau of Jiangxi, China (No. GJJ10494).

References

[1] H. Zollinger, Colour Chemistry – Synthesis, Properties of Organic Dyes and Pigments, VCH Publishers, New York, 1987.
[2] S.H. Lin, C.F. Peng, Treatment of textile wastewater by electrochemical method, Water Res. 28 (1994) 277–282.
[3] G. McMullan, C. Meehan, A. Conneely, N. Kirby, T. Robinson, P. Nigam, I.M. Banat, R. Marchant, W.F. Smyth, Microbial decolourisation and degradation of textile dyes, Appl. Microbiol. Biotechnol. 56 (2001) 81–87.
[4] I.A. Balcioglu, I. Arslan, M.T. Sacan, Homogenous and heterogenous advanced oxidation of two commercial reactive dyes, Environ. Technol. 2222 (2001) 813–822.
[5] R. Jiang, H.Y. Zhu, X.D. Li, L. Xiao, Visible light photocatalytic decolourization of C. I. Acid Red 66 by chitosan capped CdS composite nanoparticles, Chem. Eng. J. 152 (2009) 537–542.
[6] A. Kamari, W.S. Wan Ngah, M.Y. Chong, M.L. Cheah, Sorption of acid dyes onto GLA and H_2SO_4 cross-linked chitosan beads, Desalination 249 (2009) 1180–1189.
[7] H.Y. Zhu, R. Jiang, L. Xiao, Adsorption of an anionic azo dye by chitosan/kaolin/γ-Fe_2O_3 composites, Appl. Clay Sci. 48 (2010) 522–526.
[8] G.M. Walker, L.R. Weatherley, Adsorption of acid dyes on to granular activated carbon in fixed beds, Water Res. 31 (1997) 2093–2101.
[9] B.K. Nandi, A. Goswami, M.K. Purkait, Removal of cationic dyes from aqueous solutions by kaolin: kinetic and equilibrium studies, Appl. Clay Sci. 42 (2009) 583–590.
[10] C.A.P. Almeida, N.A. Debacher, A.J. Downs, L. Cottet, C.A.D. Mello, Removal of methylene blue from colored effluents by adsorption on montmorillonite clay, J. Collid Interface Sci. 332 (2009) 46–53.
[11] C. Namasivayam, R.T. Yamuna, D. Aras, Removal of Procion Orange from wastewater by adsorption on waste red mud, Sep. Purif. Technol. 37 (2002) 2421–2431.
[12] G. McKay, M.S. Otterburn, J.A. Aga, Fullers earth and fired clay as adsorbents for dyestuffs – equilibrium and rate studies, Water, Air, Soil Pollut. 24 (1985) 307–322.
[13] G. Crini, P.M. Badot, Application of chitosan, a natural aminopolysaccharide, for dye removal from aqueous solution by adsorption processes using batch studies: a review of recent literature, Prog. Polym. Sci. 33 (2008) 399–447.
[14] G.Z. Kyzas, N.K. Lazaridis, Reactive and basic dyes removal by sorption onto chitosan derivatives, J. Colloid Interface Sci. 331 (2009) 32–39.
[15] V. Singha, A.K. Sharma, D.N. Tripathi, R. Sanghi, Poly(methylmethacrylate) grafted chitosan: an efficient adsorbent for anionic azo dyes, J. Hazard. Mater. 161 (2009) 955–966.
[16] Konaganti, V. Kumar, Kota, Adsorption of anionic dyes on chitosan grafted poly(alkyl methacrylate)s, Chem. Eng. J. 158 (3) 393–401.
[17] S. Elkholy, K.D. Khalil, M.Z. Elsabee, M. Ewels, Grafting of vinyl acetate onto chitosan and biocidal activity of the graft copolymers, J. Appl. Polym. Sci. 103 (2007) 1651–1663.
[18] Y.C. Chang, S.W. Chang, D.H. Chen, Magnetic chitosan nanoparticles: studies on chitosan binding and adsorption of Co(II) ions, React. Funct. Polym. 66 (2006) 335–341.
[19] L.M. Zhou, J.P. Xu, X.Z. Liang, Z.R. Liu, Adsorption of platinum(IV) and palladium(II) from aqueous solution by magnetic cross-linking chitosan nanoparticles modified with ethylenediamine, J. Hazard. Mater. (2009) 439–446.
[20] G.A. Latha, K.B. George, G.K. Kannan, N.K. Ninan, Synthesis of a polyacrylamide chelating resin and applications in metal ion extractions, J. Appl. Polym. Sci. 43 (1991) 1159–1163.
[21] M. Monier, D.M. Ayad, Y. Wei, A.A. Sarhan, Adsorption of Cu(II), Co(II), and Ni(II) ions by modified magnetic chitosan chelating resin, J. Hazard. Mater. 177 (2010) 962–970.
[22] I. Langumuir, The adsorption of gases on plane surfaces of glass, mica and platinum, J. Am. Chem. Soc. 40 (1918) 1361–1403.
[23] H.M.F. Freundlich, Over the adsorption in solution, Z. Phys. Chem A57 (1906) 358–471.
[24] S.P. Ramnani, S. Sabharwal, Adsorption behaviour of Cr(VI) onto radiation crosslinked chitosan and its possible application for the treatment of wastewater containing Cr(VI), React. Funct. Polym. 66 (2006) 902–909.
[25] A.H. Chen, S.M. Chen, Biosorption of azo dyes from aqueous solution by glutaraldehyde-crosslinked chitosans, J. Hazard. Mater. 172 (2009) 1111–1121.
[26] A.J. Varma, S.V. Deshpande, J.F. Kennedy, Metal complexation by chitosan and its derivatives: a review, Carbohydr. Polym. 55 (2004) 77–93.

[27] M.S. Chiou, P.Y. Ho, H.Y. Li, Adsorption of anionic dyes in acid solutions using chemically cross-linked chitosan beads, Dyes Pigments 60 (2004) 69–84.
[28] Y.C. Wong, Y.S. Szeto, W.H. Cheung, G. McKay, Equilibrium studies for acid dye adsorption onto chitosan, Langmuir 19 (2003) 7888–7894.
[29] M.S. Chiou, G.S. Chuang, Competitive adsorption of dye Metanil Yellow and RB15 in acid solution on chemically cross-linked chitosan beads, Chemosphere 62 (2006) 731–740.
[30] S. Chatterjee, S. Chatterjee, B.P. Chatterjee, A.K. Guha, Adsorptive removal of congo red, a carcinogenic textile dye by chitosan hydrobeads: binding mechanism, equilibrium and kinetics, Colloids Surf. A: Physicochem. Eng. Aspects 299 (2007) 146–152.
[31] L. Qi, Z. Xu, Lead sorption from aqueous solutions on chitosan nanoparticles, Colloids Surf. A 251 (2004) 186–193.
[32] J. Tellinghuisen, Van't Hoff analysis of K (T): how good or bad? Biophys. Chem. 120 (2006) 114–120.